Dynamic Phase Alignment in Inertial Alfvén Turbulence

Lucio M. Milanese* and Nuno F. Loureiro
Plasma Science and Fusion Center, Massachusetts Institute of Technology, Cambridge, Massachusetts 02139, USA

Maximilian Daschner
Plasma Science and Fusion Center, Massachusetts Institute of Technology, Cambridge, Massachusetts 02139, USA and ETH Zurich, CH-8093 Zürich, Switzerland

Stanislav Boldyrev
Department of Physics, University of Wisconsin-Madison, Madison, Wisconsin 53706, USA and Space Science Institute, Boulder, Colorado 80301, USA

(Received 1 July 2020; revised 20 October 2020; accepted 21 October 2020; published 21 December 2020)

In weakly collisional plasma environments with sufficiently low electron beta, Alfvénic turbulence transforms into inertial Alfvénic turbulence at scales below the electron skin depth, $k_\perp d_e \gtrsim 1$. We argue that, in inertial Alfvénic turbulence, both energy and generalized kinetic helicity exhibit direct cascades. We demonstrate that the two cascades are compatible due to the existence of a strong scale dependence of the phase alignment angle between velocity and magnetic field fluctuations, with the phase alignment angle scaling as $\cos\alpha_k \propto k_\perp^{-1}$. The kinetic and magnetic energy spectra scale as $\propto k_\perp^{-5/3}$ and $\propto k_\perp^{-11/3}$, respectively. As a result of the dual direct cascade, the generalized helicity spectrum scales as $\propto k_\perp^{-5/3}$, implying progressive balancing of the turbulence as the cascade proceeds to smaller scales in the $k_\perp d_e \gg 1$ range. Turbulent eddies exhibit a phase-space anisotropy $k_\parallel \propto k_\perp^{5/3}$, consistent with critically balanced inertial Alfvén fluctuations. Our results may be applicable to a variety of geophysical, space, and astrophysical environments, including the Earth's magnetosheath and ionosphere, solar corona, and nonrelativistic pair plasmas, as well as to strongly rotating nonionized fluids.

DOI: 10.1103/PhysRevLett.125.265101

Introduction.—Many important turbulent plasma environments are characterized by a low ratio of the electron plasma pressure to magnetic energy density, that is, low β_e, in addition to weak collisionality. Examples are the ionosphere [1,2], the Earth's magnetosheath [3], the solar corona [4,5], and some instances of the solar wind [6,7]. Turbulence may play a role in structure formation, energy dissipation, magnetic reconnection, heat conduction, and other processes relevant for the dynamics and thermodynamics of such systems [6,8–16]. Despite vigorous investigation, the nature of turbulent fluctuations in low beta regimes remains incompletely understood and continues to attract considerable interest [3,17–20].

At scales below the electron skin depth in plasmas with sufficiently low β_e, the dominant low-frequency plasma modes are arguably nonlinear inertial Alfvén waves, whose turbulent cascade is governed by the existence of two ideal invariants: energy and generalized kinetic helicity. Turbulent dynamics in the presence of two invariants is poorly understood in both plasmas and nonionized fluids [21,22]. It is possible that both invariants are subject to a forward (direct) cascade or that one of them cascades forward and the other backward [20–25]. When both quantities cascade forward, one can argue in favor of the cascade of either invariant setting the nonlinear eddy turnover time [22], greatly complicating the analysis and leading to different predictions and understanding of the underlying turbulent dynamics.

In this Letter, we propose that, in inertial Alfvén turbulence, both energy and (kinetic) helicity cascade forward, and it is the cascade of energy, rather than that of helicity, that determines the cascade time. We demonstrate that, rather remarkably, this is achieved via a strongly scale-dependent *phase alignment* between fluctuations of electric and magnetic potentials, which manages to suppress helicity while allowing the energy cascade to proceed unhindered. Our phenomenological model predicts the spectra of magnetic, kinetic, and helicity fluctuations in the inertial kinetic regime, shown here to be in good agreement with the results of numerical simulations.

More broadly, we conjecture that the phenomenon of scale-dependent phase alignment uncovered in this work may be the mechanism underpinning the joint forward cascade of two ideal invariants in other physical systems, including nonconducting fluids described by the Navier–Stokes equation [22,24,26,27].

Model equations.—We consider a plasma permeated by a strong magnetic field, $B_0\hat{z}$, such that the total field is

TABLE I. Summary of different regimes of applicability of the adopted model equations.

Physical system	Asymptotic regime	Range of scales	Examples
Electron-ion plasmas	$\beta_i \ll m_e/m_i$, $\beta_e \ll m_e/m_i$	All scales	Ionospheric plasmas [1,2]
Electron-ion plasmas (inertial kinetic Alfvén waves)	$\beta_i \sim 1$, $\beta_e \ll 1$ $\omega < k_\perp v_{\rm thi}$ [3]	$k_\perp^2 d_e^2 \gg 1 + 2/\beta_i$	Regions of solar wind and corona [4–6], Earth's magnetosheath [3]
Electron-ion plasmas (inertial whistler waves)	$\beta_i \sim 1$, $\beta_e \ll 1$ $\omega > k_\perp v_{\rm thi}$ [3]	$k_\perp^2 d_e^2 \gg 1$	Regions of solar wind and corona [4–6], Earth's magnetosheath [3]
Electron-positron (pair) plasmas	$\beta \ll 1$	All scales	Upcoming low-temperature laboratory pair plasmas [41,42]
Rapidly rotating nonconducting fluids	$\omega_z \ll \Omega$	Low Rossby number $Ro \ll 1$	Low Rossby number (Ro) geophysical flows [43]

$\boldsymbol{B} = B_0\hat{z} + \delta\boldsymbol{B}_\perp$, with $\delta B_\perp/B_0 \ll 1$. The evolutionary equations that we adopt are as follows:

$$\frac{\partial}{\partial t}\nabla_\perp^2\phi + \{\phi, \nabla_\perp^2\phi\} = \{\psi, \nabla_\perp^2\psi\} + V_A\frac{\partial}{\partial z}\nabla_\perp^2\psi + f_\phi, \quad (1)$$

$$\frac{\partial}{\partial t}(1 - d_e^2\nabla_\perp^2)\psi + \{\phi, (1 - d_e^2\nabla_\perp^2)\psi\} = V_A\frac{\partial\phi}{\partial z} + f_\psi. \quad (2)$$

Here, ϕ denotes the stream function, related to the $\boldsymbol{E}\times\boldsymbol{B}$ flow velocity by $\boldsymbol{v}_\perp = \hat{z}\times\boldsymbol{\nabla}_\perp\phi$, and ψ is the flux function, related to the perpendicular component of the magnetic field by $\delta\boldsymbol{B}_\perp/\sqrt{4\pi\rho} = \hat{z}\times\boldsymbol{\nabla}_\perp\psi$, with ρ the mass density. The Poisson bracket is defined as $\{A,B\} = \partial_x A\partial_y B - \partial_x B\partial_y A$, the Alfvén speed is $V_A = B_0/\sqrt{4\pi\rho}$, and f_ϕ and f_ψ are forcing terms to be described later. The only kinetic effect included in these equations is the electron inertia, characterized by d_e, the electron skin depth [28].

These equations describe low beta nonrelativistic pair plasmas [31], as well as electron-ion plasmas in the "ultralow" beta limit, $\beta_e \sim \beta_i \ll m_e/m_i$ [32]. The modes described by these equations are (as we show below) the inertial Alfvén modes. However, quite importantly, our equations are also pertinent to a wide range of other environments. When $k_\perp^2 d_e^2 \gg 1 + 2/\beta_i$, our equations are structurally identical to Eqs. (19) and (20) of Ref. [3], which were derived under the assumptions of $\beta_i \sim 1$ and $\beta_e \ll 1$. The dominant low-frequency modes there are inertial kinetic Alfvén waves ($\omega < k_\perp v_{\rm thi}$, with $v_{\rm thi}$ the ion thermal speed) [3,33]. In addition, in the limit $k_\perp^2 d_e^2 \gg 1 + 2/\beta_i$, Eqs. (1) and (2) are structurally equivalent to Eqs. (25) and (26) of Ref. [3], which describe inertial whistler waves ($\omega > k_\perp v_{\rm thi}$) in reduced electron magnetohydrodynamics (MHD). One can also demonstrate that, quite remarkably, in the limit $k_\perp^2 d_e^2 \gg 1$, our equations map onto the equations describing rapidly rotating nonionized fluids [34]. A short derivation of Eqs. (1) and (2) is presented in the Supplemental Material [35], while a summary of their regimes of applicability is shown in Table I. In the Supplemental Material, which includes Refs. [36–40], we also discuss the instrumental resolution required to measure turbulent fluctuations in the $k_\perp^2 d_e^2 \gg 1$ range in space plasmas.

Equations (1) and (2) have two quadratic invariants: total energy,

$$\mathcal{E} = \frac{1}{2}\int dV\{(\nabla_\perp\psi)^2 + d_e^2(\nabla_\perp^2\psi)^2 + (\nabla_\perp\phi)^2\}, \quad (3)$$

and generalized kinetic helicity,

$$\mathcal{H} = \int dV\{\nabla_\perp^2\phi(1 - d_e^2\nabla_\perp^2)\psi\}, \quad (4)$$

which reduces to cross-helicity at MHD scales ($k_\perp d_e \ll 1$).

The only linear mode supported by these equations is the inertial Alfvén wave, with dispersion relation and eigenfunctions given by

$$\omega_l = \pm\frac{k_z V_A}{\sqrt{1 + k_\perp^2 d_e^2}}, \qquad \phi = \pm\sqrt{1 + k_\perp^2 d_e^2}\,\psi. \quad (5)$$

Inertial Alfvén turbulence.—The focus of our Letter is on turbulence in the kinetic range $k_\perp d_e \gg 1$. In the opposite limit of $k_\perp d_e \ll 1$, Eqs. (1) and (2) become the reduced MHD (RMHD) equations [44–46], and thus the results obtained for RMHD are expected to apply [47]. Following Ref. [31], the energy flux at scales $k_\perp d_e > 1$ is expected to be $\varepsilon \sim k_\perp^2\phi_\lambda^2/\tau_\lambda$, where τ_λ is the eddy turnover time at the scale $\lambda \sim k_\perp^{-1}$, and $\tau_\lambda = 1/\omega_{\rm nl} \sim 1/(k_\perp^2\phi_\lambda)$. This yields $\phi_\lambda \sim \varepsilon^{1/3}k_\perp^{-4/3}$, leading to the scaling of the spectrum of perpendicular kinetic energy $\mathcal{E}_K(k_\perp)dk_\perp \sim \varepsilon^{2/3}k_\perp^{-5/3}dk_\perp$. For $k_\perp^2 d_e^2 \gg 1$, equipartition between parallel and perpendicular kinetic energies, i.e., between the second and third terms in Eq. (3), results in $\psi_\lambda \sim k_\perp^{-7/3}$, from which follows the magnetic energy spectrum $\mathcal{E}_B(k_\perp)dk_\perp \sim \varepsilon^{2/3}k_\perp^{-11/3}dk_\perp$. Finally, postulating critical balance of the fluctuations in this range (i.e., that the characteristic linear and nonlinear frequencies of the system approximately balance at each scale [46,48]) yields

$$k_\parallel \sim \varepsilon^{1/3} d_e V_A^{-1} k_\perp^{5/3}. \quad (6)$$

Using the above scalings for ϕ_λ and ψ_λ, we would predict the helicity spectrum to scale as $\mathcal{H}(k_\perp)dk_\perp \sim k_\perp^{-2/3} dk_\perp$ in the kinetic range. However, as discussed in Ref. [31], in this case the helicity flux cannot be constant; rather it should *increase* at small scales, leading to a contradiction. If, on the other hand, we assume that the scaling of the fields should be determined by a direct helicity cascade, we would formally conclude that the energy cannot cascade toward small scales at $k_\perp d_e > 1$. This contradiction can be solved if, as conjectured in Ref. [31], the helicity flux at scales $k_\perp d_e \gg 1$ is written as

$$(k_\perp^2 \phi_\lambda)(d_e^2 k_\perp^2 \psi_\lambda) R_\lambda / \tau_\lambda \sim \varepsilon_H, \quad (7)$$

where R_λ is a scale-dependent cancellation factor. Requiring that the flux of kinetic helicity be constant in the kinetic range and enforcing consistency between energy and helicity fluxes leads to

$$R_\lambda \sim \varepsilon_H (k_\perp^2 \phi_\lambda)^{-2} (d_e^2 k_\perp^2 \psi_\lambda)^{-1} \sim \varepsilon_H (k_\perp d_e)^{-1}. \quad (8)$$

When the cancellation factor is present, the simultaneous direct cascades of *both* energy and helicity become possible, and we arrive at a different prediction for the helicity spectrum, $\mathcal{H}(k_\perp)dk_\perp \sim k_\perp^{-5/3} dk_\perp$. In what follows we demonstrate that the cancellation factor is a manifestation of a new phenomenon that we call *"dynamic phase alignment"*: an increasing correlation between the *phases* of the fluctuating magnetic and velocity fields as the cascade progresses toward smaller scales.

Numerical setup.—We now report on direct numerical simulations carried out to test these theoretical predictions. We integrate Eqs. (1) and (2) with the code VIRIATO [49] on a triply periodic domain using a grid of $N_\perp^2 \times N_\parallel$ points. Hyperdissipation terms of the form $\nu_H \nabla_\perp^6$ are included on the right-hand side of both equations, with ν_H set to remove energy at the grid scale. Energy is injected via delta-correlated forcing terms of the form

$$f_{\phi,\psi} = C_{\phi,\psi} \alpha_\pm \delta(k_x - k_{x0}) \delta(k_y - k_{y0}) \cos(k_{z0} z), \quad (9)$$

where C_ϕ and C_ψ are randomly chosen complex numbers determining the phase of the mode being excited ($C_\phi \neq C_\psi$ and $|C_{\phi,\psi}| = 1$), and $\alpha_\pm > 0$ are numerical coefficients determining the strength of the drive, their subscript relating to positive and negative (generalized) kinetic helicity injection, as discussed below. The mode numbers k_{x0}, k_{y0}, and k_{z0} are randomly chosen from a predetermined range and at every time step they are the same for both f_ϕ and f_ψ.

From Eqs. (4) and (9), one can show that the kinetic helicity injected at any time step by the forcing terms is given by

TABLE II. Summary of key simulation parameters.

ID	$N_\perp$	$N_\parallel$	$(k_\perp d_e)_{\min}$	$\mathcal{R}_\mathcal{H}$
A1	2048	2048	0.02	10
B1	768	4096	0.3	1
B2	768	4096	0.3	30

$$\mathcal{H}_{\text{inj}}^\pm \propto k_{\perp 0}^2 (1 + k_{\perp 0}^2 d_e^2) \alpha_\pm^2 \text{Re}[C_\phi C_\psi], \quad (10)$$

where $k_{\perp 0}^2 = k_{x0}^2 + k_{y0}^2$. When $\text{Re}[C_\phi C_\psi] > 0$, i.e., when the phase between f_ϕ and f_ψ is such that positive helicity is injected at a particular time step, the α_+ coefficient is used in the forcing terms. When $\text{Re}[C_\phi C_\psi] < 0$, the coefficient α_- is used instead. We define the ratio of positive to negative kinetic helicity injection as $\mathcal{R}_\mathcal{H} \equiv \mathcal{H}_{\text{inj}}^+ / \mathcal{H}_{\text{inj}}^-$. The ratio of the coefficients is set as $\alpha_+ / \alpha_- = \sqrt{\mathcal{R}_\mathcal{H}}$.

Table II summarizes key parameters of the simulations performed. In all cases, energy is injected at the largest scales, where $k_\perp d_e < 1$. In runs A1 and B2, net positive kinetic helicity is injected by the forcing terms ($\mathcal{R}_\mathcal{H} = 10$ and $\mathcal{R}_\mathcal{H} = 30$, respectively), while in run B1 no *net* kinetic helicity is injected ($\mathcal{R}_\mathcal{H} = 1$). Run A1 aims at capturing the dynamics in both the RMHD and kinetic range and providing insight into how the transition between the two regimes occurs. Simulations of type B aim at capturing in more detail the turbulent dynamics in the kinetic range.

Energy spectra.—Figure 1(a), (b) shows the energy and (generalized kinetic) helicity spectra (obtained from time-averaged data after steady state is reached) for simulation A1. The magnetic energy spectrum is seen to smoothly transition from $\sim k_\perp^{-5/3}$ to $\sim k_\perp^{-11/3}$ at $k_\perp d_e \approx 1$, whereas the kinetic energy scales as $\sim k_\perp^{-5/3}$ throughout the inertial range, as does the helicity spectrum. These observations are in good agreement with the theoretical predictions and offer an immediate confirmation of the existence of the scale-dependent cancellation factor $R_\lambda \sim 1/k_\perp$ at scales $k_\perp d_e > 1$.

Runs of type B confirm the kinetic range results over a larger scale range [see Fig. 2(b), (d)]. The energy spectra are not significantly affected by the ratio of positive to negative helicity injected in the system. When no net helicity is injected in the system, the spectrum of helicity is not well-defined [Fig. 2(b)]. One can observe that the sign of kinetic helicity is different at different perpendicular wave numbers $k_\perp$ in the inertial range, and its value is zero when spatially averaged over the entire simulation domain and time averaged over the steady state. When instead net helicity is injected in the system, a well-defined spectrum is observed, exhibiting a scaling $\sim k_\perp^{-5/3}$ [Fig. 2(d)], as in simulation A1.

To characterize eddy anisotropy, we consider that the parallel wave number of a fluctuating field ϕ at perpendicular scale $k_\perp$ may be approximated as [50]

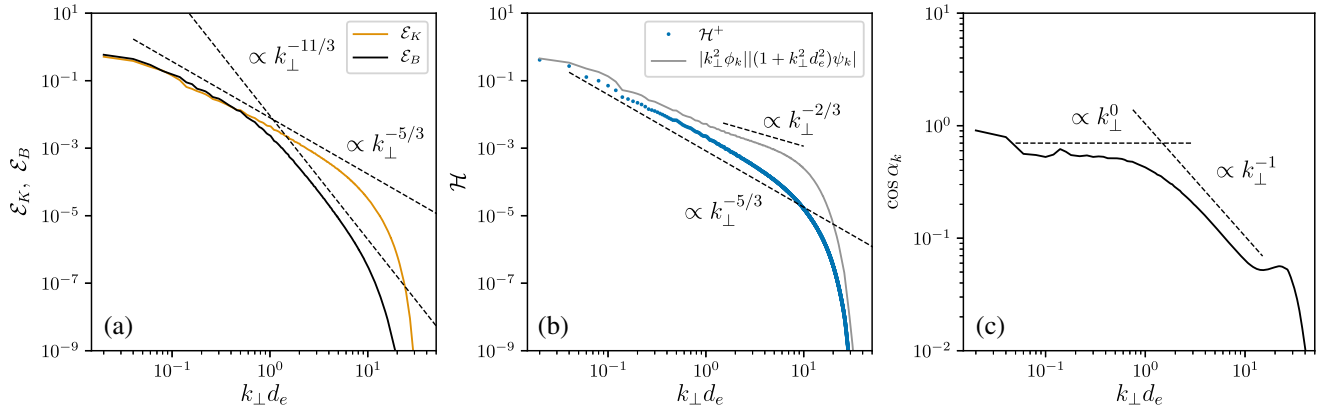

FIG. 1. Simulation A1. (a) Spectra of magnetic and kinetic energy. (b) Spectra of kinetic helicity and of the product of the absolute value of the factors in the integrand of Eq. (4). (c) Scale dependence of the average phase angle between fluctuations of electric and magnetic potential in Fourier space.

$$k_\parallel \approx \left(\frac{\langle|\boldsymbol{B}_0\partial_z\phi_{k_\perp}+\delta\boldsymbol{B}_{k_\perp}\cdot\boldsymbol{\nabla}\phi_{k_\perp}|^2\rangle}{\langle B_{k_\perp}^2\rangle\langle\phi_{k_\perp}^2\rangle}\right)^{1/2}, \tag{11}$$

where $\langle\ldots\rangle$ denotes spatial averaging. In the kinetic range, electromagnetic fluctuations are small because electron inertia ($k_\perp^2 d_e^2\partial_t\psi$) dominates over the inductive part of the electric field ($\partial_t\psi$) in Eq. (2). Therefore, turbulence in this regime is essentially electrostatic, i.e., $\boldsymbol{B}_0\partial_z\phi_{k_\perp}\gg\delta\boldsymbol{B}_{k_\perp}\cdot\boldsymbol{\nabla}\phi_{k_\perp}$, and thus $k_\parallel\approx k_z$. The scatter plots in Fig. 2(a), (c) show, for each value of k_z, the corresponding value of $k_\perp$ at which the energy of the ϕ fluctuations is largest. The data exhibit the scaling $k_\parallel\propto k_\perp^{5/3}$, in agreement with Eq. (6), confirming that the inertial Alfvén cascade is critically balanced [3].

Kinetic helicity spectrum and dynamic phase alignment.—The net kinetic helicity at each wave number is a function of the absolute value of the Fourier coefficients $|\phi_k|$ and $|\psi_k|$, and of the phase angle between them, α_k. For a given $k_\perp$, the average value of α_k is given by

$$\cos\alpha_k=\frac{1}{2}\frac{\langle k_\perp^2\phi_{k\perp}(1+d_e^2k_\perp^2)\psi_{k\perp}^*+\text{c.c.}\rangle}{\langle|k_\perp^2\phi_{k\perp}||(1+d_e^2k_\perp^2)\psi_{k\perp}|\rangle}, \tag{12}$$

where the numerator represents net kinetic helicity at a given perpendicular wave number. In the $k_\perp d_e<1$ range,

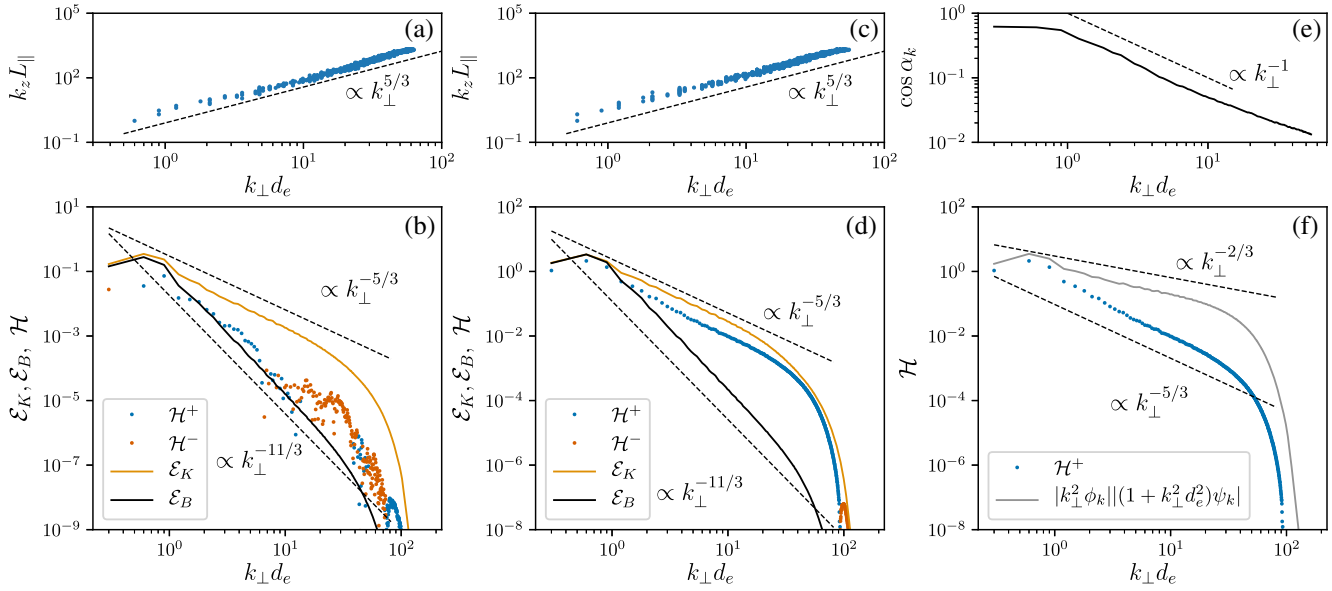

FIG. 2. Eddy anisotropy scaling for simulations B1 and B2 [subplots (a) and (c), respectively]. Spectra of kinetic helicity and of kinetic and magnetic energy for simulations B1 and B2 [subplots (b) and (d), respectively]. Different colors are used to represent the presence of net positive or negative helicity in perpendicular wave-number shells. Subplot (f) presents the spectra of kinetic helicity and of the product of the absolute value of the factors in the integrand of Eq. (4) in simulation B2. The corresponding average value of the cosine of the phase angle [Eq. (12)] as a function of scale is shown in subplot (e).

the spectra of $|k_\perp^2\phi_{k\perp}||\psi_{k\perp}|$ and of generalized kinetic helicity (which turns into cross helicity at such scales) are both expected to exhibit the scaling of the MHD energy spectrum, and thus $\cos\alpha_k$ should not depend strongly on scale. At scales $k_\perp d_e > 1$, however, the spectrum of $|k_\perp^2\phi_{k\perp}||k_\perp^2 d_e^2\psi_{k\perp}|$ is expected to scale as $k_\perp^{-2/3}$, while we predict, and observe, kinetic helicity to scale as $k_\perp^{-5/3}$. We thus expect $\cos\alpha_k \propto k_\perp^{-1}$. This is confirmed in Fig. 1(c): in the RMHD range, $\cos\alpha_k$ does not vary strongly as a function of scale. After a smooth transition at $k_\perp d_e \approx 1$, the scaling of $\cos\alpha_k$ asymptotes to $\propto k_\perp^{-1}$ for $k_\perp d_e > 1$. Figure 2(e) confirms the scaling $\cos\alpha_k \propto k_\perp^{-1}$ in the kinetic range.

When $\cos\alpha_k = 0$, kinetic helicity is zero and the system is in a perfectly balanced state. The scaling $\cos\alpha_k \propto k_\perp^{-1}$ therefore implies that the turbulence becomes progressively more balanced as the cascade proceeds deeper in the kinetic range. This statement is corroborated by results included in the Supplemental Material [35], where we present an analysis of the scale-dependent probability density function of generalized kinetic helicity density (h).

Conclusions.—In this Letter, we showed that, in inertial Alfvén turbulence, both energy and generalized kinetic helicity cascade forward, with the cascade of energy determining the nonlinear eddy turnover time. Helicity is found to scale as $\mathcal{H} \propto k_\perp^{-5/3}$ in the kinetic range, a result that is underpinned by a scale-dependent alignment angle, $\cos\alpha_k \propto k_\perp^{-1}$, between the Fourier phases of magnetic and velocity fields. Consequently, turbulence becomes progressively more balanced as the cascade proceeds deeper into the kinetic range.

The results presented in this Letter may be valuable for interpreting the direct measurements of low beta turbulence in space plasmas [4–7], as well as for other astrophysical and geophysical turbulent systems where dual energy and kinetic helicity cascades are possible (e.g., subrelativistic pair plasma [31], whose experimental realization is upcoming [41,42]; ionospheric [1,2] and magnetospheric plasmas [3]; and strongly rotating nonconducting fluids [43]). Another context where our findings may be pertinent is Navier–Stokes (NS) turbulence. Simulations reveal a $k^{-5/3}$ scaling of kinetic helicity and a scale-dependent progressive balancing of turbulence (restoration of mirror symmetry) [24,26,27] whose underlying dynamics is not fully understood. We conjecture that the novel mechanism of dynamic phase alignment uncovered in this work may also be at play in NS turbulence and account for those results. While the details of the nonlinear interactions in plasma and NS turbulence are different, our conjecture is based on commonalities between particular aspects of the joint forward cascade of energy and (generalized) kinetic helicity. In particular, in both systems, a "naïve" estimate of the spectral scaling of helicity, without the inclusion of a scale-dependent phase alignment factor, would yield a scaling $\sim k^{-2/3}$, which, if realized, would prevent energy from cascading forward. In both systems, a scaling $\mathcal{H} \sim k^{-5/3}$ is instead observed [24,27], which may be underpinned, in the case of NS turbulence, by a scale-dependent alignment between the phases of velocity and vorticity fluctuations.

Work supported by DOE Award No. DE-FG02-91ER54109 (L. M. M. and N. F. L.), NSF CAREER Grant No. 1654168 and NSF CAREER Grant No. 2010136 (N. F. L.), the Prof. Amar G. Bose Research Fellows Program at MIT (L. M. M. and N. F. L.), and NSF Grant No. PHY-1707272, NASA Grant No. 80NSSC18K0646, and DOE Award No. DESC0018266 (S. B.). This research used resources of the facilities of the Massachusetts Green High-Performance Computing Center (MGHPCC) and of the National Energy Research Scientific Computing Center (NERSC), a U.S. Department of Energy Office of Science User Facility operated under Contract No. DE-AC02-05CH11231.

*Corresponding author.
milanese@mit.edu

[1] C. K. Goertz and B. W. Boswell, Magnetosphere-ionosphere coupling, J. Geophys. Res. **84**, 7239 (1979).
[2] A. Kumari, R. P. Sharma, and N. Yadav, Inertial Alfven wave induced turbulent spectra in aurora, Astrophys. Space Sci. **351**, 81 (2014).
[3] C. H. K. Chen and S. Boldyrev, Nature of kinetic scale turbulence in the Earth's magnetosheath, Astrophys. J. **842**, 122 (2017).
[4] M. J. Aschwanden, A. I. Poland, and D. M. Rabin, The new solar corona, Annu. Rev. Astron. Astrophys. **39**, 175 (2001).
[5] S. R. Cranmer, Coronal holes, Living Rev. Solar Phys. **6**, 3 (2009).
[6] C. W. Smith, D. J. Mullan, N. F. Ness, R. M. Skoug, and J. Steinberg, Day the solar wind almost disappeared: Magnetic field fluctuations, wave refraction and dissipation, J. Geophys. Res. **106**, 18625 (2001).
[7] C. H. Chen, L. Leung, S. Boldyrev, B. A. Maruca, and S. D. Bale, Ion-scale spectral break of solar wind turbulence at high and low beta, Geophys. Res. Lett. **41**, 8081 (2014).
[8] P. L. Similon and R. N. Sudan, Plasma turbulence, Annu. Rev. Fluid Mech. **22**, 317 (1990).
[9] D. Biskamp, *Magnetohydrodynamic Turbulence* (Cambridge University Press, Cambridge, England, 2003).
[10] T. D. Phan *et al.*, Electron magnetic reconnection without ion coupling in Earth's turbulent magnetosheath, Nature (London) **557**, 202 (2018).
[11] C. Vega, V. Roytershteyn, G. L. Delzanno, and S. Boldyrev, Electron-only reconnection in kinetic-Alfvén turbulence, Astrophys. J. **893**, L10 (2020).
[12] J. E. Stawarz, J. P. Eastwood, T. D. Phan, I. L. Gingell, M. A. Shay, J. L. Burch, R. E. Ergun, B. L. Giles, D. J. Gershman, O. L. Contel, P.-A. Lindqvist, C. T. Russell, R. J. Strangeway, R. B. Torbert, M. R. Argall, D. Fischer, W. Magnes, and L. Franci, Properties of the turbulence

associated with electron-only magnetic reconnection in Earth's magnetosheath, Astrophys. J. **877**, L37 (2019).
[13] P. Sharma Pyakurel, M. A. Shay, T. D. Phan, W. H. Matthaeus, J. F. Drake, J. M. TenBarge, C. C. Haggerty, K. G. Klein, P. A. Cassak, T. N. Parashar, M. Swisdak, and A. Chasapis, Transition from ion-coupled to electron-only reconnection: Basic physics and implications for plasma turbulence, Phys. Plasmas **26**, 082307 (2019).
[14] L. V. Kozak, V. A. Pilipenko, O. M. Chugunova, and P. N. Kozak, Statistical analysis of turbulence in the foreshock region and in the Earth's magnetosheath, Cosmic Res. (Transl. of Kosm. Issled.) **49**, 194 (2011).
[15] C. P. Wang, M. Gkioulidou, L. R. Lyons, and V. Angelopoulos, Spatial distributions of the ion to electron temperature ratio in the magnetosheath and plasma sheet, J. Geophys. Res. **117**, 1 (2012).
[16] K. Iwai, K. Shibasaki, S. Nozawa, T. Takahashi, S. Sawada, J. Kitagawa, S. Miyawaki, and H. Kashiwagi, Coronal magnetic field and the plasma beta determined from radio and multiple satellite observations, Earth, Planets Space **66**, 1 (2014).
[17] E. A. Lucek, D. Constantinescu, M. L. Goldstein, J. Pickett, J. L. Pinçon, F. Sahraoui, R. A. Treumann, and S. N. Walker, The magnetosheath, Space Sci. Rev. **118**, 95 (2005).
[18] F. Sahraoui, S. Y. Huang, G. Belmont, M. L. Goldstein, A. Rétino, P. Robert, and J. De Patoul, Scaling of the electron dissipation range of solar wind turbulence, Astrophys. J. **777**, 15 (2013).
[19] R. S. Hughes, S. P. Gary, and J. Wang, Particle-in-cell simulations of electron and ion dissipation by Whistler turbulence: Variations with electron β, Astrophys. J. **835**, L15 (2017).
[20] T. Passot, P. L. Sulem, and E. Tassi, Gyrofluid modeling and phenomenology of low-βe Alfvén wave turbulence, Phys. Plasmas **25**, 042107 (2018).
[21] W. H. Matthaeus, M. Wan, S. Servidio, A. Greco, K. T. Osman, S. Oughton, and P. Dmitruk, Intermittency, nonlinear dynamics and dissipation in the solar wind and astrophysical plasmas, Phil. Trans. R. Soc. A **373**, 20140154 (2015).
[22] A. Alexakis and L. Biferale, Cascades and transitions in turbulent flows, Phys. Rep. **767–769**, 1 (2018).
[23] A. Brissaud, U. Frisch, J. Leorat, M. Lesieur, and A. Mazure, Helicity cascades in fully developed isotropic turbulence, Phys. Fluids **16**, 1366 (1973).
[24] Q. Chen, S. Chen, G. L. Eyink, and D. D. Holm, Intermittency in the Joint Cascade of Energy and Helicity, Phys. Rev. Lett. **90**, 214503 (2003).
[25] J. J. Podesta and A. Bhattacharjee, Theory of incompressible magnetohydrodynamic turbulence with scale-dependent alignment and cross-helicity, Astrophys. J. **718**, 1151 (2010).
[26] G. Sahoo, M. De Pietro, and L. Biferale, Helicity statistics in homogeneous and isotropic turbulence and turbulence models, Phys. Rev. Fluids **2**, 024601 (2017).
[27] A. Pouquet, D. Rosenberg, J. E. Stawarz, and R. Marino, Helicity dynamics, inverse, and bidirectional cascades in fluid and magnetohydrodynamic turbulence: A brief review, Earth Space Sci. **6**, 351 (2019).
[28] The dispersion relation for inertial Alfvén waves, Eq. (5), implies that $\omega_l/|k_z| \gg v_{\rm the}$ at scales $k_\perp \rho_e \ll 1$, where $\rho_e = m_e c v_{\rm the}/eB_0$ is the electron Larmor radius. Since low β_e implies $d_e \gg \rho_e$, we find that electron Landau damping may thus be neglected at scales $d_e > k_\perp^{-1} \gg \rho_e$, where the resonant condition is not satisfied. This is unlike $\beta_e \sim 1$ plasmas, in which $d_e \sim \rho_e$ and where, therefore, electron Landau damping may be expected to play an important role at electron scales [29,30].
[29] F. Sahraoui, M. L. Goldstein, P. Robert, and Y. V. Khotyaintsev, Evidence of a Cascade and Dissipation of Solar-Wind Turbulence at the Electron Gyroscale, Phys. Rev. Lett. **102**, 231102 (2009).
[30] O. Alexandrova, C. H. Chen, L. Sorriso-Valvo, T. S. Horbury, and S. D. Bale, Solar wind turbulence and the role of ion instabilities, Space Sci. Rev. **178**, 101 (2013).
[31] N. F. Loureiro and S. Boldyrev, Turbulence in magnetized pair plasmas, Astrophys. J. **866**, L14 (2018).
[32] A. Zocco and A. A. Schekochihin, Reduced fluid-kinetic equations for low-frequency dynamics, magnetic reconnection, and electron heating in low-beta plasmas, Phys. Plasmas **18**, 102309 (2011).
[33] S. Boldyrev and N. F. Loureiro, Role of reconnection in inertial kinetic-Alfvén turbulence, Phys. Rev. Research **1**, 012006 (2019).
[34] K. Julien and E. Knobloch, Reduced models for fluid flows with strong constraints, J. Math. Phys. (N.Y.) **48**, 065405 (2007).
[35] See Supplemental Material at http://link.aps.org/supplemental/10.1103/PhysRevLett.125.265101 for a short derivation of the adopted model equations and of equations describing the dynamics of rotating, nonconducting fluids in strongly anisotropic regimes. We also present further evidence supporting the existence of a scale-dependent balancing of turbulence at scales $k_\perp d_e > 1$ and we briefly discuss the instrumental resolution required to measure turbulent fluctuations in the $k_\perp^2 d_e^2 \gg 1$ range in space plasmas.
[36] P. Louarn, J. E. Wahlund, T. Chust, H. de Feraudy, A. Roux, B. Holback, P. O. Dovner, A. I. Eriksson, and G. Holmgren, Observation of kinetic Alfvén waves by the FREJA spacecraft, Geophys. Res. Lett. **21**, 1847 (1994).
[37] C. E. Seyler, J.-E. Wahlund, and B. Holback, Theory and simulation of low-frequency plasma waves and comparison to Freja satellite observations, J. Geophys. Res. **100**, 21453 (1995).
[38] K. Stasiewicz, Y. Khotyaintsev, M. Berthomier, and J. E. Wahlund, Identification of widespread turbulence of dispersive Alfvén waves, Geophys. Res. Lett. **27**, 173 (2000).
[39] D. Verscharen, K. G. Klein, and B. A. Maruca, The multi-scale nature of the solar wind, Living Rev. Solar Phys. **16**, 5 (2019).
[40] M. Maksimovic *et al.*, The solar orbiter radio and plasma waves (RPW) instrument, Astron. Astrophys. **642**, A12 (2020).
[41] E. V. Stenson, S. Nißl, U. Hergenhahn, J. Horn-Stanja, M. Singer, H. Saitoh, T. S. Pedersen, J. R. Danielson, M. R. Stoneking, M. Dickmann, and C. Hugenschmidt, Lossless Positron Injection into a Magnetic Dipole Trap, Phys. Rev. Lett. **121**, 235005 (2018).

[42] J. Horn-Stanja, E. V. Stenson, M. R. Stoneking, M. Singer, U. Hergenhahn, S. Nißl, H. Saitoh, S. Pedersen, M. Dickmann, C. Hugenschmidt, and J. R. Danielson, Injection of intense low-energy reactor-based positron beams into a supported magnetic dipole trap, Plasma Res. Express **2**, 015006 (2020).

[43] S. V. Nazarenko and A. A. Schekochihin, Critical balance in magnetohydrodynamic, rotating and stratified turbulence: Towards a universal scaling conjecture, J. Fluid Mech. **677**, 134 (2011).

[44] B. Kadomtsev and O. Pogutse, Nonlinear helical perturbations of a plasma in the tokamak, Sov. J. Exp. Theor. Phys. **38**, 575 (1974).

[45] H. R. Strauss, Nonlinear, three-dimensional magnetohydrodynamics of noncircular tokamaks, Phys. Fluids **19**, 134 (1976).

[46] A. A. Schekochihin, S. C. Cowley, W. Dorland, G. W. Hammett, G. G. Howes, E. Quataert, and T. Tatsuno, Astrophysical gyrokinetics: Kinetic and fluid turbulent cascades in magnetized weakly collisional plasmas, Astrophys. J. Suppl. Ser. **182**, 310 (2009).

[47] J. C. Perez, J. Mason, S. Boldyrev, and F. Cattaneo, On the Energy Spectrum of Strong Magnetohydrodynamic Turbulence, Phys. Rev. X **2**, 041005 (2012).

[48] P. Goldreich and S. Sridhar, Toward a theory of interstellar turbulence. 2: Strong alfvenic turbulence, Astrophys. J. **438**, 763 (1995).

[49] N. F. Loureiro, W. Dorland, L. Fazendeiro, A. Kanekar, A. Mallet, M. S. Vilelas, and A. Zocco, Viriato: A Fourier–Hermite spectral code for strongly magnetized fluid–kinetic plasma dynamics, Comput. Phys. Commun. **206**, 45 (2016).

[50] J. Cho and A. Lazarian, The anisotropy of electron magnetohydrodynamic turbulence, Astrophys. J. **615**, L41 (2004).